Supplement of Atmos. Chem. Phys., 24, 7983–8005, 2024
https://doi.org/10.5194/acp-24-7983-2024-supplement

Atmospheric Chemistry and Physics
Open Access
EGU

Supplement of

Vertical structure of a springtime smoky and humid troposphere over the southeast Atlantic from aircraft and reanalysis

Kristina Pistone et al.

Correspondence to: Kristina Pistone (kristina.pistone@nasa.gov)

Supplementary Material

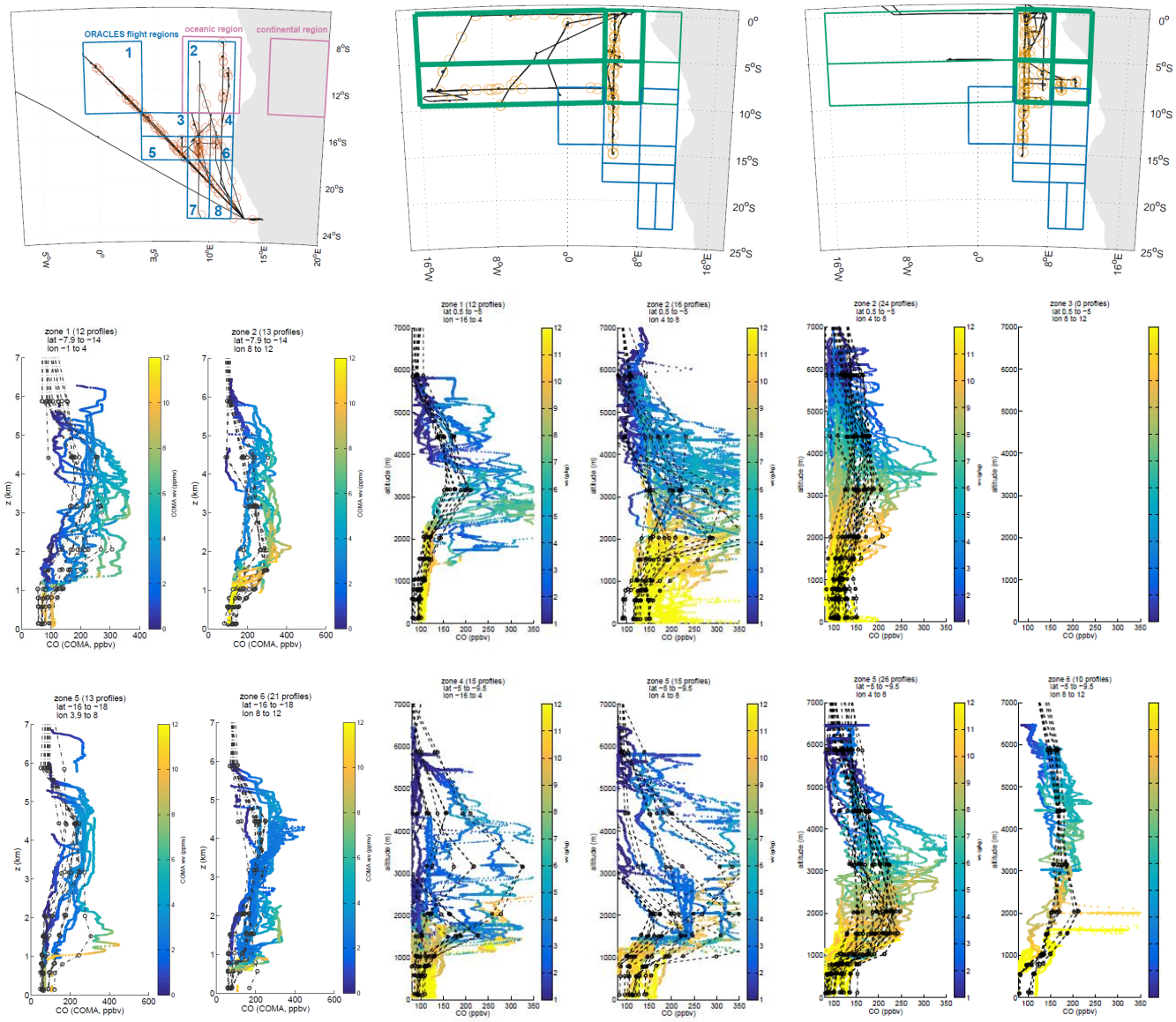

Figure S1. Sample subset of spatially subdivided CO profiles for the each ORACLES flight campaign and corresponding CAMS profiles, showing the good agreement of vertical extent and the consistent underestimation in CAMS particularly in the maximum CO values. Spatial subdivisions correspond to Regions 1-2 and 5-6 for 2016 (numbering as used in Pistone et al., 2021), and to the bolded green regions for 2017 and 2018 (also shown in Figure 1). Colors indicate the specific humidity.

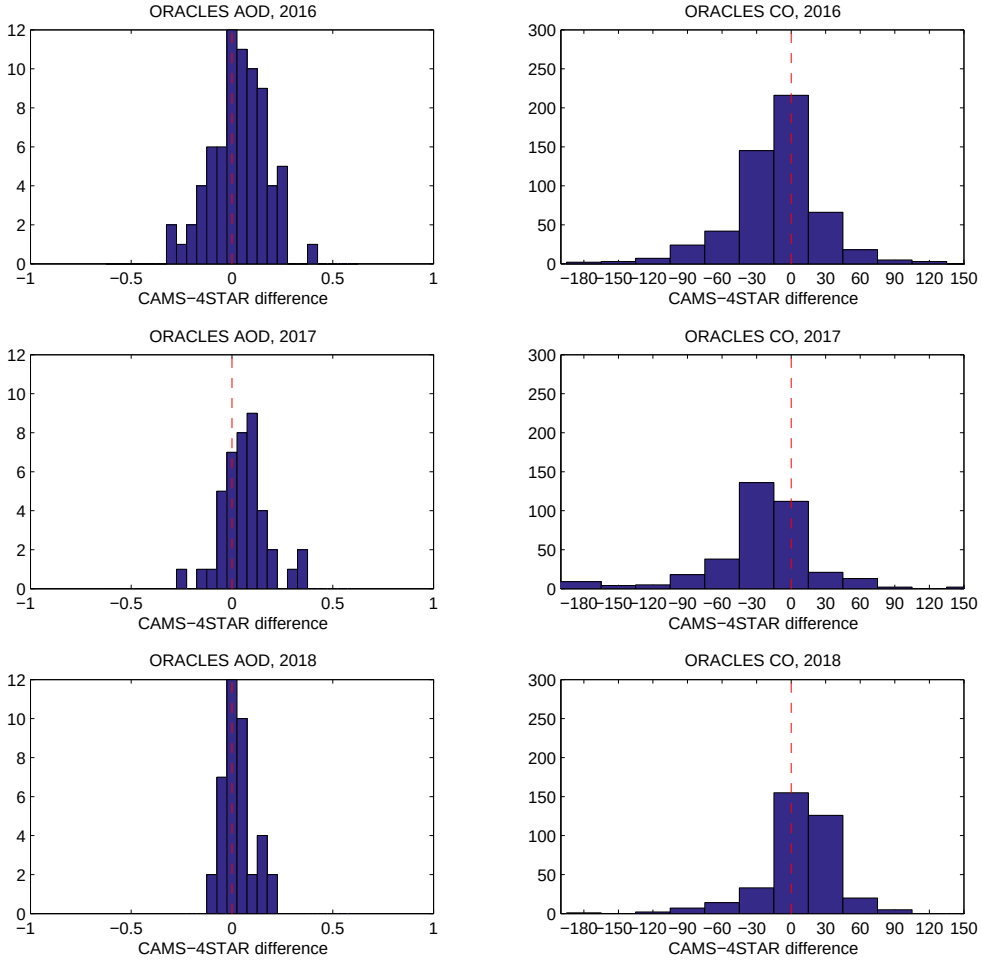

Figure S2. Difference between (left) CAMS BB AODs and ORACLES 4STAR-reported AODs and (right) CAMS CO and ORACLES COMA-measured CO for each deployment, taken at the subsets shown in Figure 6. The majority of the AODs are within ± 0.2 of one another; CAMS tends to overestimate AOD relative to 4STAR. In contrast, CAMS tends to underestimate CO relative to the observations, except in October.

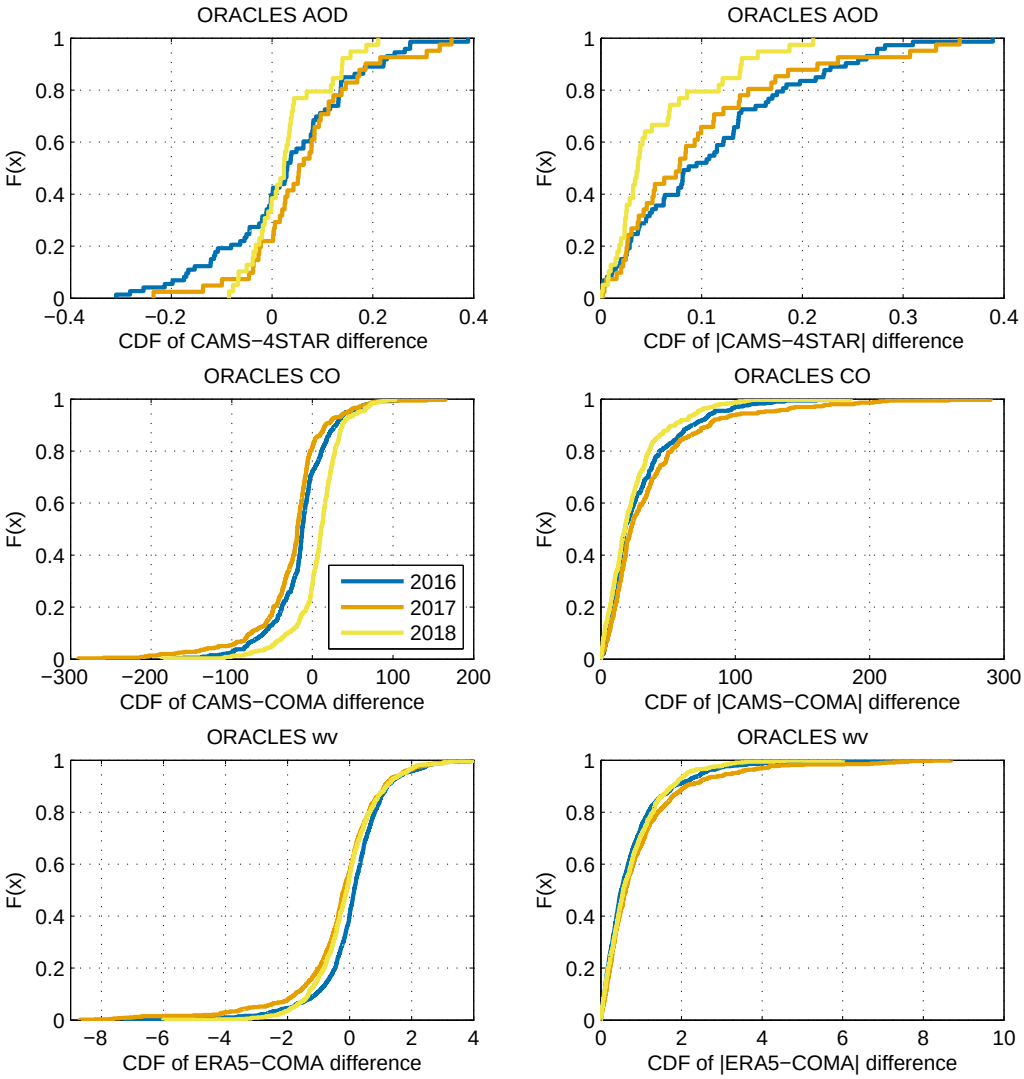

Figure S3. Cumulative distribution functions showing the agreement between collocated reanalysis-observation comparison points (differences, left, and in absolute values, right), for each deployment year. The right side shows the good absolute agreement between reanalysis and observations, especially for the vertically resolved values (i.e., CO and water vapor), and the left side shows the tendencies of these distributions towards over- vs underestimations (e.g. slight overestimation in AOD in CAMS, and slight underestimation in CO, with the exception of 2018.)

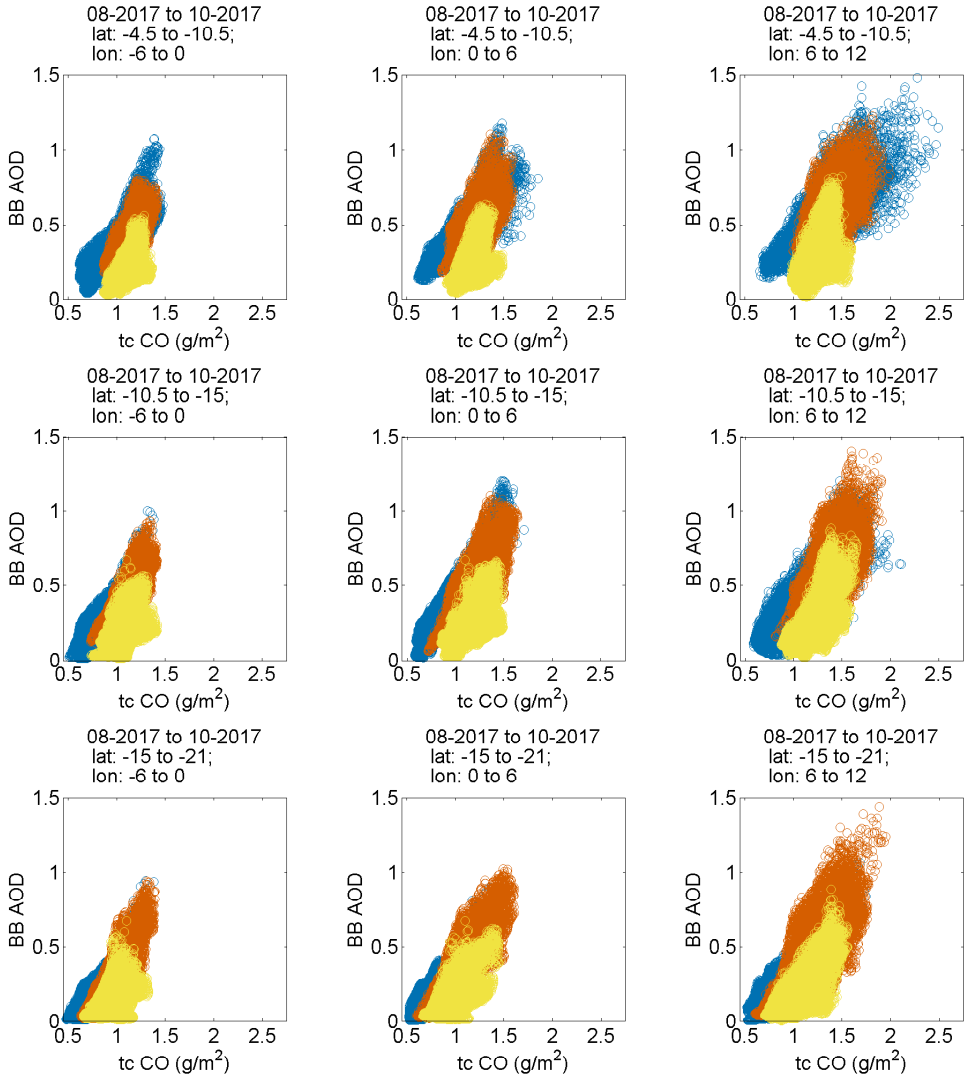

Figure S4. Gridded CAMS column total column carbon monoxide versus column biomass burning AOD (organics + BC) for 2017. August (blue) has a less steep slope than October (yellow) with September (orange) intermediate, showing the seasonal evolution of column values.

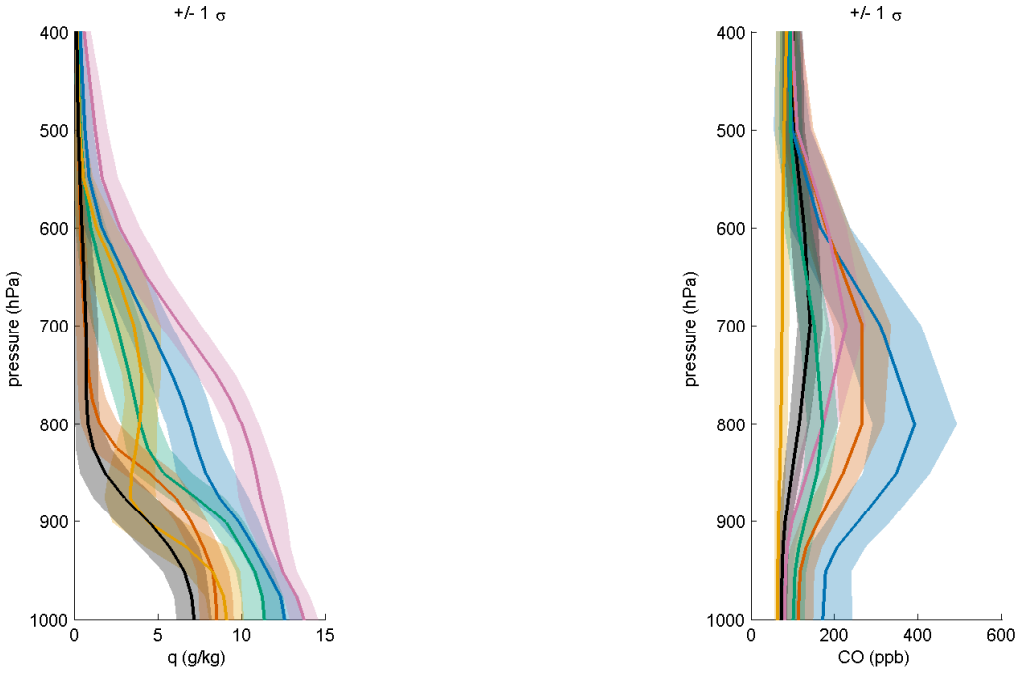

Figure S5. K-means classifications for q and CO, showing the range (standard deviation) of the ERA5 and CAMS (respectively) profiles classified as that profile type.

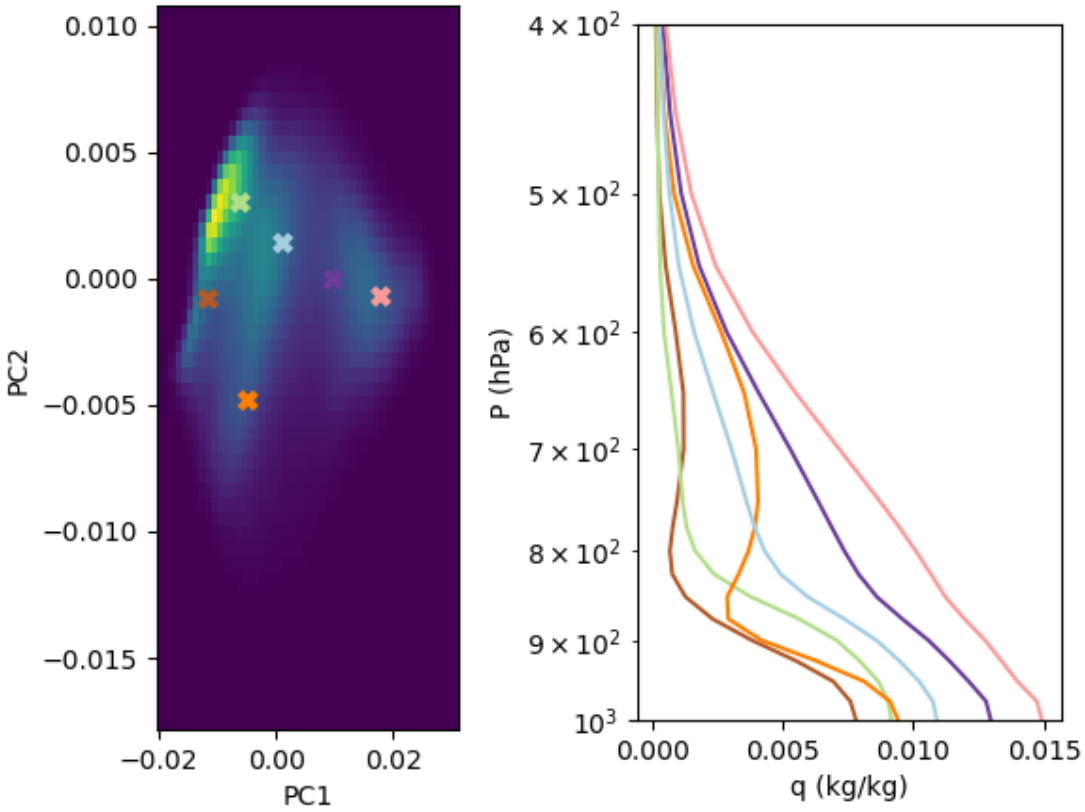

Figure S6. Principal component analysis (left panel) showing the relative abundance of water vapor profiles in ERA5 in the phase space of the first and second principal components (PC1 and PC2, respectively) of all ERA5 water vapor profiles over the region. 'X' symbols indicate the centroid locations in the phase space of the principal components of a k-means clustering analysis on abundance of water vapor profiles in the phase space. Right panel shows the resulting water vapor profiles associated with each of the 6 clusters produced from the k-means clustering analysis, which serve as the canonical set of water vapor profiles over the region shown in Figure 7.

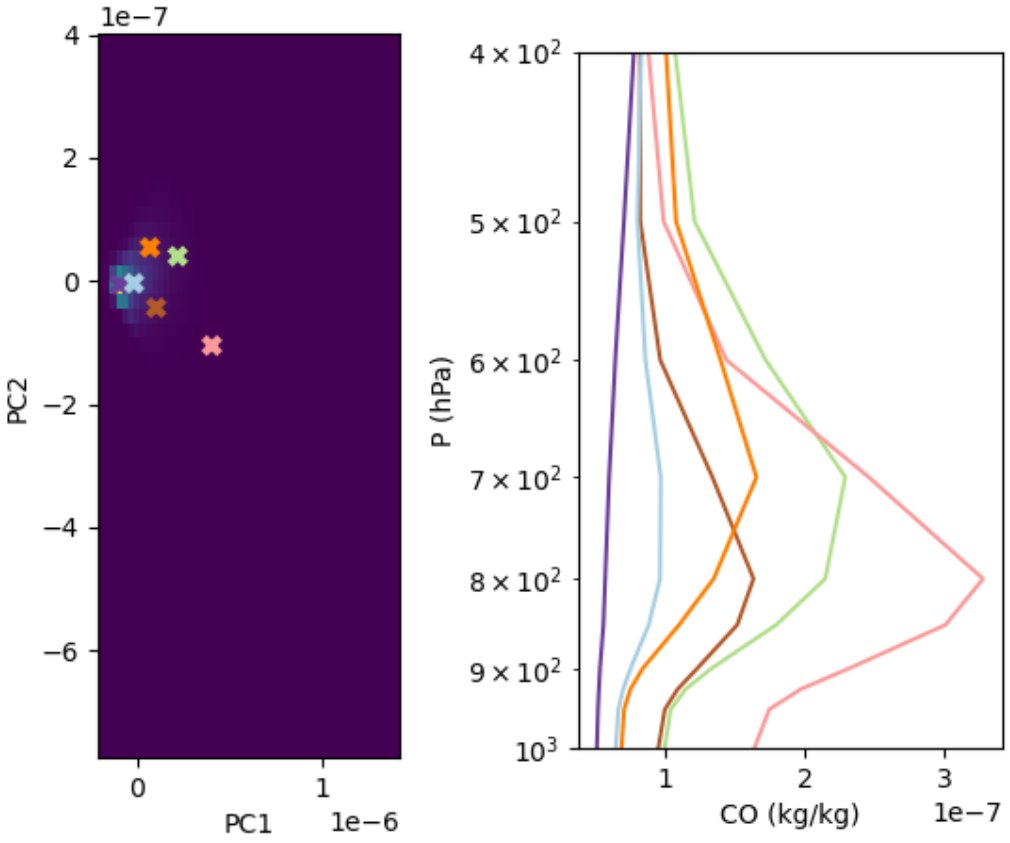

Figure S7. Same as Figure S6 but for profiles of CO from the CAMS simulations. Right panel shows the resulting CO profiles that serve as the canonical set of CO profiles shown in Figure 8

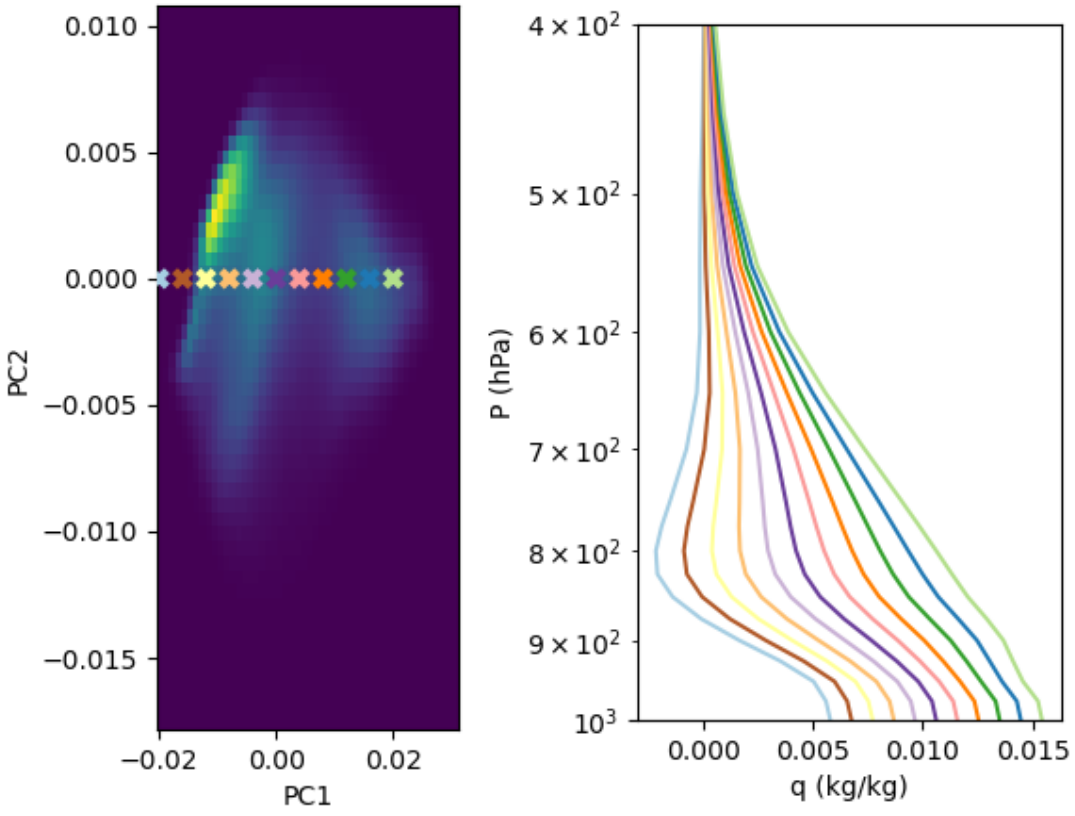

Figure S8. Left panel shading is the same as left panel in Figure S6. 'X' symbols show samples selected from across the range of values of the first principal component for a constant value of the second principal component. Right panel shows the resulting water vapor profile corresponding to each 'X' symbol and illustrates the variability of the first principal component of the water vapor profiles, which is largely showing the variation in the magnitude of the column water vapor concentration.

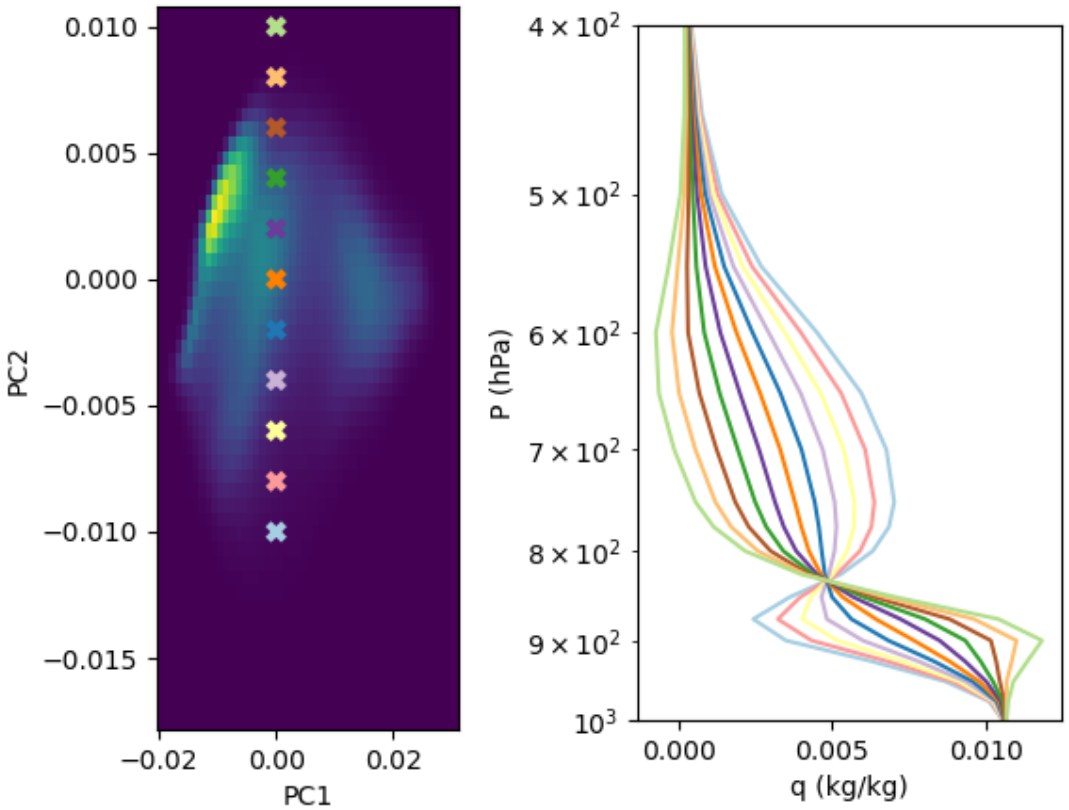

Figure S9. As in Figure S8 but the right panel illustrates the variability of the second principal component of the water vapor profiles (right panel), which is capturing the variations in upper-level q between the 500 and 800 hPa pressure levels relative to the lower-level q below the 850 hPa pressure level.

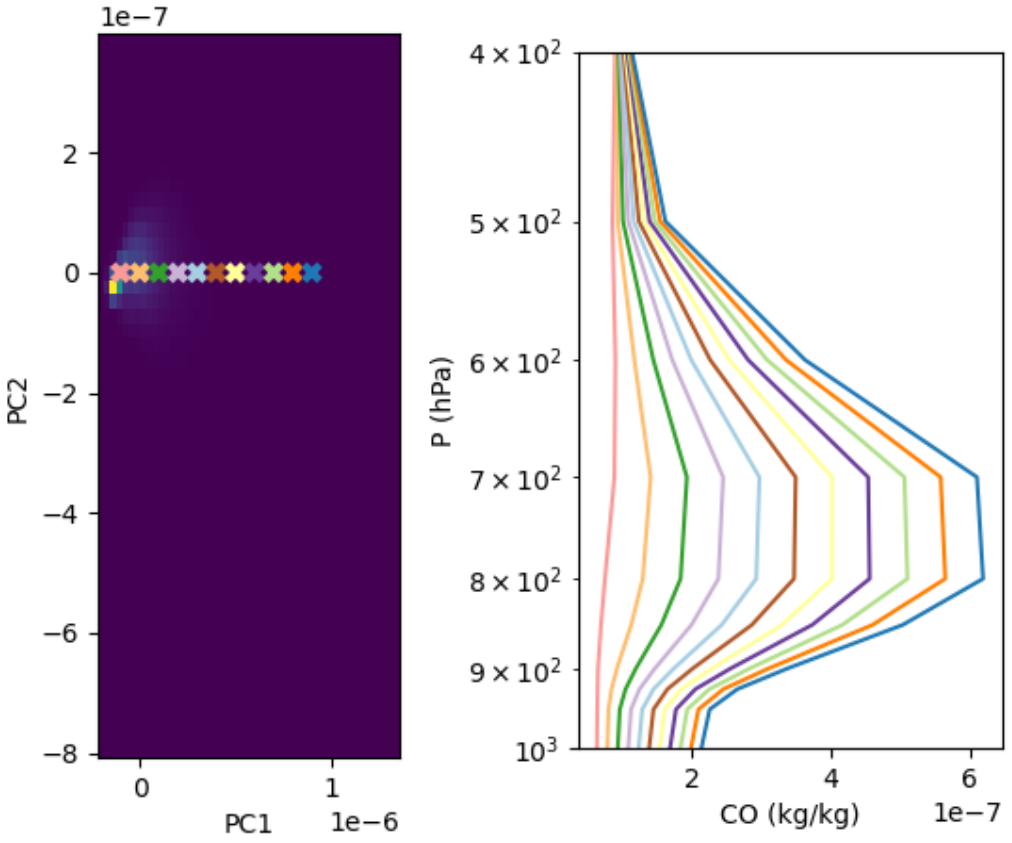

Figure S10. As in Figure S8 but the right panel illustrates the variability of the first principal component of the CO profiles, which is largely showing the variation in the magnitude of the column CO concentration.

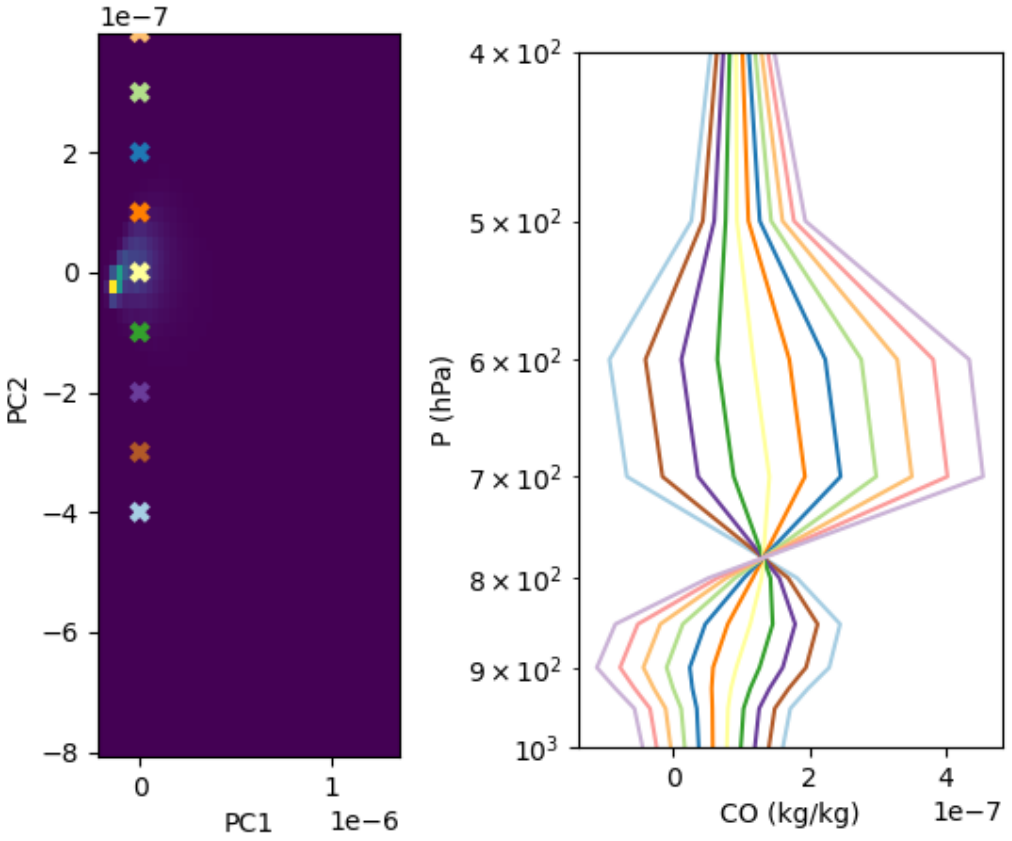

Figure S11. As in Figure S10 but the right panel illustrates the variability of the second principal component of the CO profiles, which is capturing the variations in upper-level CO concentration between the 500 and 800 hPa pressure levels relative to the lower-level CO concentration below the 800 hPa pressure level.